# Improving the Performance of the Power Supply of the Cyclotron Harmonic Coils

S. G. Ramadan and G. M. Sarhan
*High Institute of Technology*
*University of Benha*
*Benha, Kalyubia 13512, Egypt*
gamal_bhit@yahoo.com

A. A. Hagras and Sh. M. Saad
*Nuclear Research Centre*
*Egyptian Atomic Energy Authority (EAEA)*
*Abo Zaabal, Cairo 13759, Egypt*
ashrafa1973@yahoo.com &shokryms@hotmail.com

***Abstract* - Correction of lower harmonics of the cyclotron magnetic field is of great importance for its operation. Error in the magnetic field lower harmonics can reduce the efficiency of the beam extraction. For control of the cyclotron magnetic field lower harmonics, the so called inner and outer harmonic coils are provided. These harmonic coils must be fed by a very high accuracy current source power supply. This power supply must be equipped with a high resolution measurement and control scheme. Harmonic coils are supplied with conventional thyristor controlled converters with analog control strategy. Frequent interruption of operation and difficulties in the adjustment of harmonic coil current lead to economical and research - time losses. This research project aims to replace this conventional system with a more effective, accurate and less complicated digital control system based on Motorola DSP56F807 and high switching frequency power circuit.**

***Index Term - Cyclotron, DC-DC choppers, DSP applications.***

## I. INTRODUCTION

A multichannel power supply system feeds the harmonic coils with dc current to establish a magnetic field so that a vertical component of this magnetic field is excited in the median plane in the area of location of these coils. The magnetic field set by the main magnet in the central region and at the edges of the chamber has lower harmonics due to the magnet geometry. These lower harmonics result in a non uniform magnetic field and affect the circulation of the beam in these regions and, consequently, reduce the efficiency of the ion beam extraction from the cyclotron. Fig. 1 shows the location of harmonic coils inside the chamber.

Actually, stability of the acceleration process, attainment of the final energy of the accelerated beam from the cyclotron and efficiency of the beam extraction system depend on the lower harmonics control. Error in the magnetic field lower harmonics can reduce the efficiency of the beam extraction resulting in complete disappearance of the extracted beam of the cyclotron. Harmonic coils are supplied with conventional thyristor controlled converters with analog control strategy based on conventional control techniques. Frequent interruption of operation and difficulties in the adjustment of harmonic coil current lead to economical and research - time losses.

This research project aims to replace this conventional system with a more effective, accurate and less complicated digital control system based on Motorola DSP56F807 and high switching frequency power circuit. Actually all the bulky modules including the analog integrator, the signal monitoring and protection, the pulse phase modulator, normalizers, current transducer and the comparator are all replaced by a single module circuit[1-2]. This paper is organized as follows. In section II the conventional power supply was presented to shows its different components and how it is replaced by the proposed digital system which was designed in section III. Section IV presents how the system was implemented and the flow chart of the main program. Section V presents comparison between the experimental results of the proposed and the conventional systems to show the gained improvements. The conclusions were drawn in section VI.

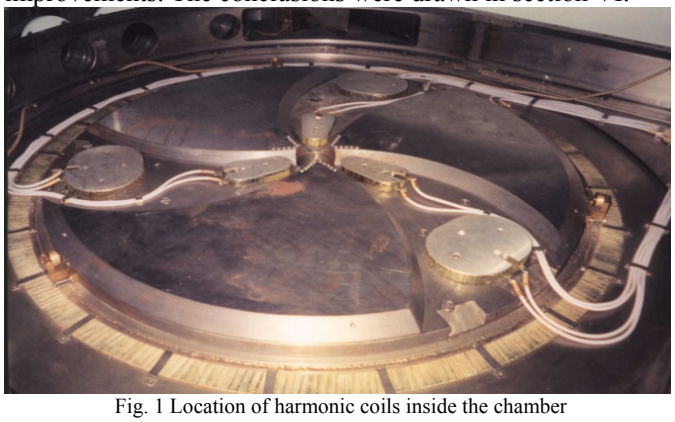

Fig. 1 Location of harmonic coils inside the chamber

## II. THE CONVENTIONAL POWER SUPPLY SYSTEM

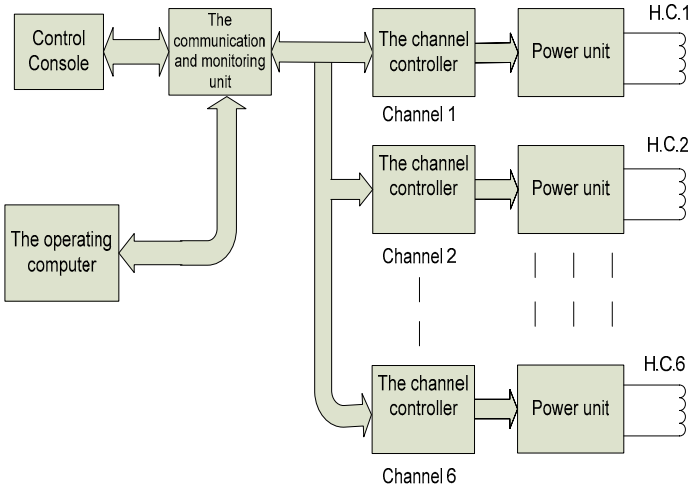


Fig. 2 Block diagram of the existing power supply system

Fig. 2 depicts the block diagram of the overall conventional power supply system. The multichannel power supply of harmonic coils consists of six channels dual power supplies of stabilized current. Every channel has a power unit and channel controller. There is a part of the power supply common to all channels. This part is the communication and monitoring unit.

In addition the system comprises the universal communication control cards, one for each channel. This card is responsible for the control and monitoring functions according to the specified program and for transmission of information on power supply operation both in the local and remote control regime [2].

*A. The power unit of the conventional power supply system*

The circuit diagram of the power unit is shown in fig. 3. The thyristor VS7 installed between the power inputs of the power amplifier transistors is triggered when voltage across VT1 is increased. This is made to protect the power amplifier transistor VT1 against inadmissible over voltages particularly dangerous at a short circuit on the load. The thyristor VS6 with the circuit R6, VD1, VD2 protects the harmonic coils against inadmissible over voltages on the power supply channel output.

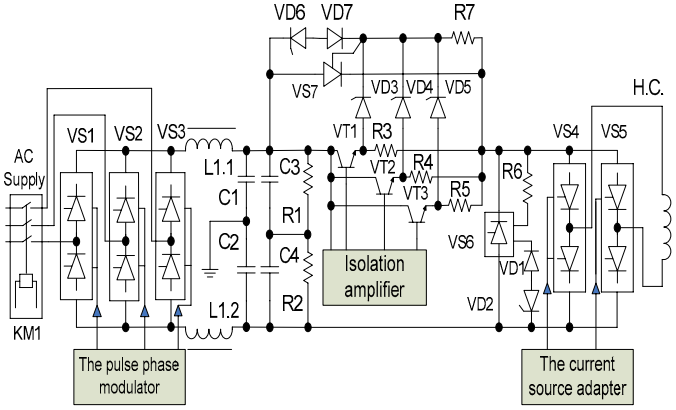


Fig. 3 The circuit diagram of the power unit of the power supply of harmonic coils

*B. The channel controller*

The channel controller consists of set of communication and control cards which comprises the following units according to fig. 4.

1- The universal communication control (U/C) card.
2- The comparison device (C.D.) (comparator) card
3- The current source adapter (C.S.A.) card.
4- The measuring current transducer (M.C.T.) card.
5- The regulator card.
6- The phase pulse modulator (P.P.M.) card.
7- The synchronization voltage normalizer (S.V.N.) card (on load).
8- The synchronization voltage normalizer (S.V.N.) card (after the passive filter).

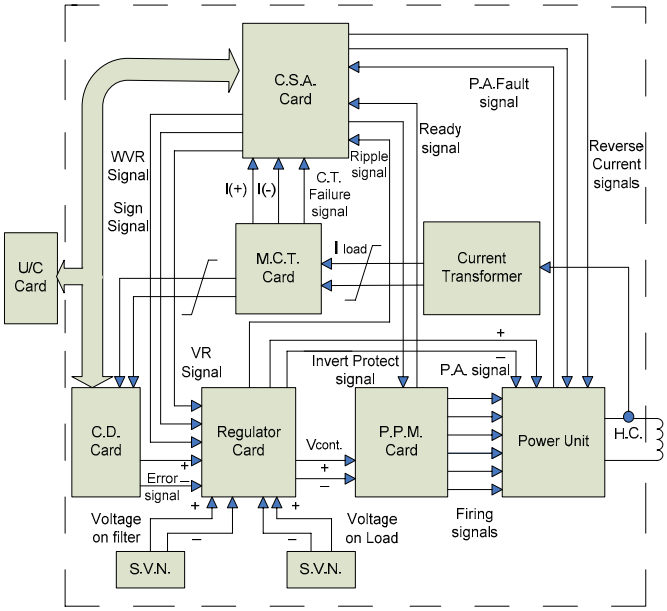


Fig. 4 The detailed block diagram for the channel controller

The power supply channel protection system is made so that all signals from sensors of controllable parameters of the power unit are collected in the current source adapter which depending on the signal type switches a channel to one of the main status of the power supply. The deblocking system in the power supply channel is made so that the circuit reset is possible only after shooting of any type of troubles, which are indicated on the front panel of the control console. Voltage feedbacks after the passive filter and on load are realized by the voltage normalizers.

## III. DESCRIBTION OF THE PROPOSED POWER SUPPLY SYSTEM

The new power supply system constitutes three compact units; the digital signal processor, precision Hall Effect current measurement module and six PWM chopper units one for each module. The general block diagram of this system is depicted in fig. 5.

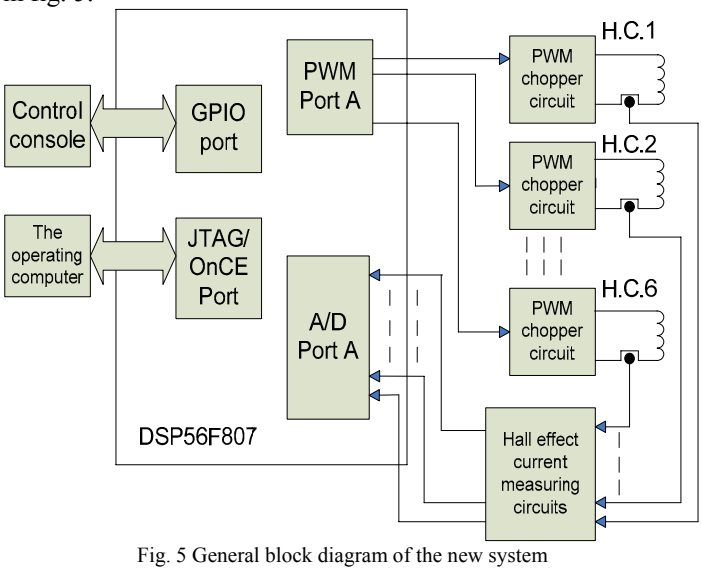


Fig. 5 General block diagram of the new system

*A. Current Measuring Circuit*

The measurement of dc load current is necessary for closed loop control. There are various methods to measure the dc load current, the traditional method for measuring that current was based on measuring the voltage drop on a small series resistor. Another method based on Hall Effect sensor is implemented in this work for the dc load current measurement as shown in fig. 6.

The current measuring circuit permits high isolation between high power and low power sides. The measured current is transformed through a Hall transducer (LA55-P) into voltage signal with a suitable scale factor, which is determined by adjusting the measuring resistor $R_M$ that provides a scale factor of 3.3V/20A. The TL081 op-amp and its adjustable offset resistor $R_{offset}$ are used as buffer to prevent loading on the measuring circuit [3].

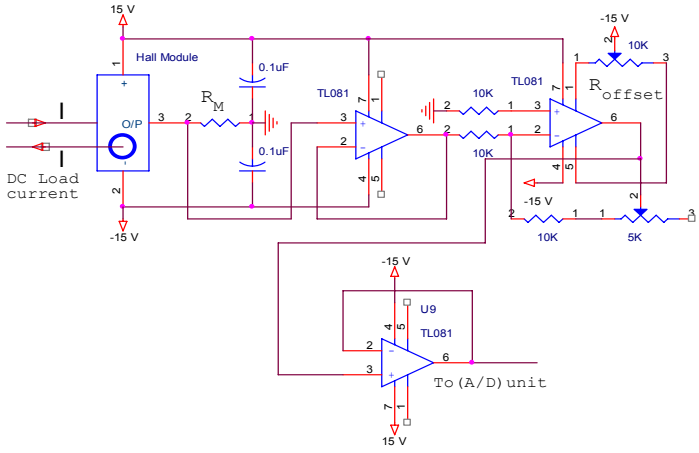


Fig. 6 Current measuring circuit

*B. The Power Circuit*

The type of power circuit capable of supplying dc current in either direction without any external switches is the four quadrant DC chopper. Fig. 7 shows the typical configuration of this chopper.

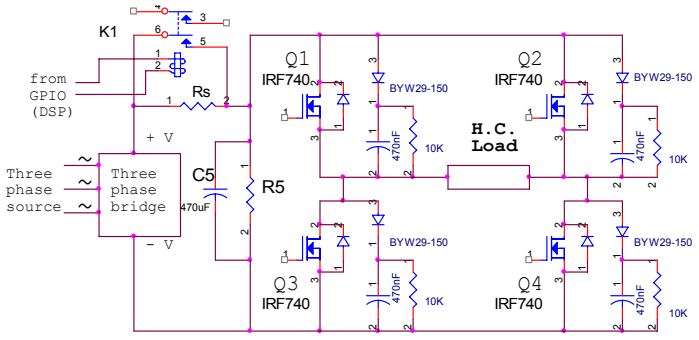


Fig. 7 Main power circuit

*C. Steady State Analysis of Step Down (buck) Chopper with RL Load*

The step down DC-DC chopper is shown in fig. 8(a) where the load is R-L. When Q1 is ON the supply voltage appears across the load and the current would increase until it reaches the steady state value expressed by $i = E_{dc} / R$.

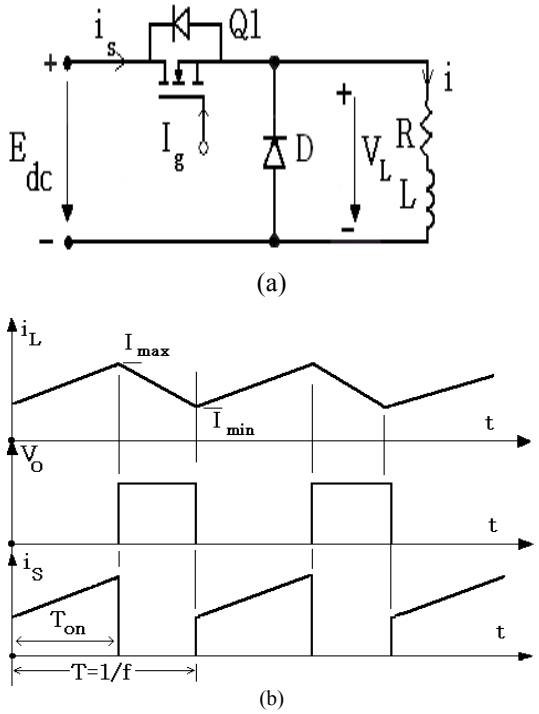


Fig. 8 Step down chopper (a) circuit diagram (b) current and voltage waveforms.

**Mode 1:** $0 < t < T_{on}$ when Q1 is turned on, current flows through the path $E_{dc+}$, R, L and $E_{dc-}$ . For this mode of operation the differential equation governing this performance is given by

$$E_{dc} = Ri + L\frac{di}{dt}, \qquad \text{For } 0 \le t \le T_{on} \qquad (1)$$

**Mode 2:** $T_{on} \le t \le T$ when Q1 is off, the load current continuously flowing through the freewheeling diode in Q2. For this mode of operation, the differential equation governing its performance is given by

$$0 = Ri + L\frac{di}{dt}, \qquad \text{For } T_{on} \le t \le T \qquad (2)$$

By taking inverse Laplace transforms and making substitutions we can get:

$$I_{pp} = I_{max} - I_{min}$$

$$= \frac{E_{dc}}{R}\frac{(1 - e^{-KT/\tau})(1 - e^{-(1-KT)/\tau})}{1 - e^{-T/\tau}} \qquad (3)$$

Where $I_{pp}$ is the peak to peak ripple and k is the duty cycle. This equation shows a number of important features of the ripple current.

-The ripple current reduces to zero as k approaches 0 and 1.

-Differentiation of eq. (3) reveals that the max. ripple current $\hat{I}_{pp}$ occurs at k=0.5.

-The longer the load L/R time constant, the lower the output ripple current $I_{pp}$.

-The higher the switching frequency, 1/T, the lower the output ripple.

### D. *Design of the Snubber Circuit*

Snubbers enhance the performance of the switching circuits and result in higher reliability, higher efficiency, higher switching frequency, smaller size, lower weight, and lower EMI. The purpose of RCD (resistance, capacitor and diode) snubber used in clamp mode is different from one used in the rate of rise control mode. In clamp mode the objective is to keep the switch from exceeding some maximum voltage. The switch itself will have to sustain the peak power dissipation of turning off. Only the peak voltage will be limited. The prime characteristic of the snubber which distinguishes the clamp mode from the rate of rise control mode is the RC time constant which is much longer than the switching period in the clamp mode. The circuit shown in fig. 9 cannot be used for rate of rise control mode since there is a DC path through the snubber. To function properly the resistor value must be large [4].

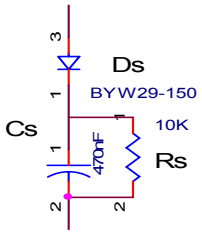


Fig. 9 The RCD clamp snubber

### E. *Heat Sink Design*

Switching losses in MOSFET's tend to be very low at frequencies below 50 kHz and therefore may be neglected, along with gate and off state losses. The first step in thermal design is to determine the total power dissipation in the device which is generally dominated by the conduction loss. Since the switching frequency and duty cycle are both relatively high the thermal resistance concept based on average junction power dissipation is valid. Assuming zero losses other than conduction losses.

$$P_d = P_c = I_d{}^2 R_{ds(on)}(25°C)[1+\alpha(T_{j\max}-25°C)] \quad (4)$$

Where $P_d$ :The total dissipated losses, $P_c$ :The conduction losses, $I_d$ : The drain current, $R_{ds\,(on)}$ : The on state drain to source resistance , $T_{j\max}$ : is the maximum junction operating temperature and $\alpha$ : is the temperature coefficient of the on state resistance of the MOSFET and is typically 1 percent.

$$T_{j\max} = T_a + R_{\theta j-a} P_d \quad (5)$$

Where $R_{\theta j-a}$ is the junction to ambient thermal resistance. From datasheet of the MOSFET IRF740, $T_{j\max}$ = 150 °C, $R_{ds\,(on)}$ (25 °C) = 0.45 ohm and the ambient temperature $T_a$ =25 °C.

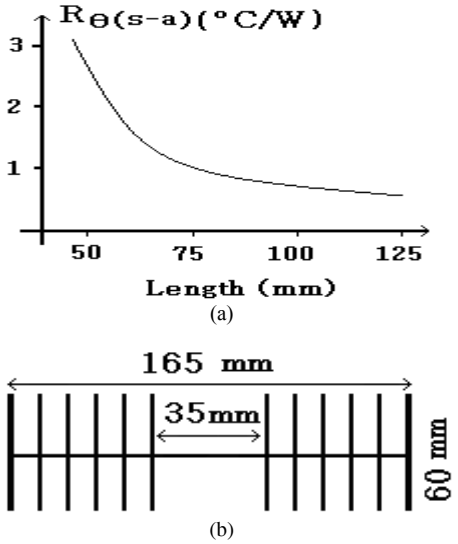


Fig. 10 Heat sink typical data

To design a finned type heat sink as shown in fig. 10(b) with length = 75 mm. then from fig. 10(a), $R_{\theta(s-a)}$ (the sink to ambient thermal resistance) = 1° C/W. From datasheet of the MOSFET IRF740, $R_{\theta(j-c)}$ (the junction to case thermal resistance) =1° C/W. If we do not use mica insulator and silicon grease is absent then $R_{\theta(c-s)}$ (the case to sink thermal resistance) = 2.5 ° C/W. Consequently $R_{\theta(j-a)} = R_{\theta(j-c)} + R_{\theta(c-s)} + R_{\theta(s-a)}$ = 4.5°C/W.

Substituting in (5) gives $P_d$ = 27.8 watts and substituting for $I_d$ in (4) results $I_d$ = 5.25A. From datasheet of MOSFET IRF 740 the maximum current at ($T_a$ = 25 ° C) = 5A and to achieve the maximum current 20A in the harmonic coils we must use four MOSFET's in parallel and every MOSFET has the same heat sink [5].

## IV. SOFTWARE SET UP OF THE SYSTEM

In this work, software implementation of the system is based on digital signal processor DSP56F807, which contains different facilities that are studied and experimented individually using simple programs [6,7]. These facilities are the following:

- *Analog to Digital Converter Unit (A/D)*
- *Pulse Width Modulation Unit (PWM)*
- *General Purpose Input Output Unit (GPIO)*

### A. *Implementation of Load Current Closed Loop Control*

The software algorithm of the closed loop control shown in fig. 11 can be described as follows:

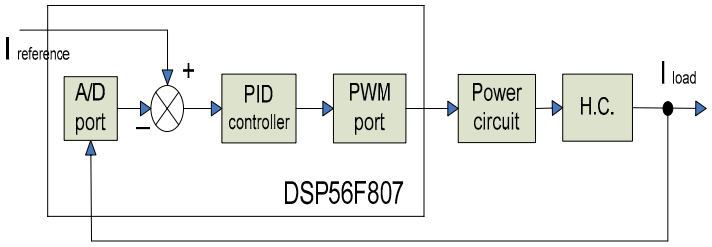


Fig. 11 Load current closed loop control

The actual load current is measured through the measuring circuit and compared with the reference current, and the resulting error signal is applied to the PI controller to produce the control signal of the MOSFET transistor.

*B. Software Algorithm of the Main Program*

The main program includes the following sections:

*1) Definition and initialization of variables:* There are many variables need to be defined and initialized in registers at the beginning of the software program such as actual and reference currents, gains of the controller and PWM frequency.

*2) Configuration of A/D unit:* The ADC unit was configured for single sequential configuration and single ended connection. All optional interrupts zero crossing, low limit, high limit and end of scan interrupts was disabled.

*3) Calculating the PI controller output:* The PI algorithm will be designed to achieve improved transient response with zero steady state error and stable dc load current.

*4) Configuration of PWM unit to produce the PWM signal output:* The PWM unit was configured for independent channel operation and edge aligned pulse width control to load the desired PWM frequency, which achieves the minimum ripples in the dc load current. The flowchart of the main program is shown in fig. 12.

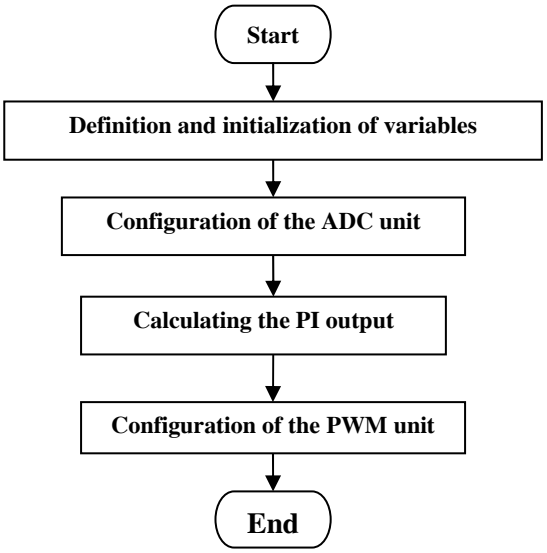


Fig. 12 Flow chart of the main program

## V. EXPERIMENTAL RESULTS

Results of the experimental work are demonstrated for closed loop control system. The controller is practically tuned to obtain the optimal parameters of the PI controller. The experimental results of the conventional power supply system are also presented to compare with that of the new system to show the obtained improvements. The experimental prototype of buck chopper is supplied from 24V three phase voltage source that was rectified to 54Vdc. The chopper circuit has current rating 20A, equals to the maximum load current of harmonic coils.

*A. Experimental Results of the Conventional Power Supply System*

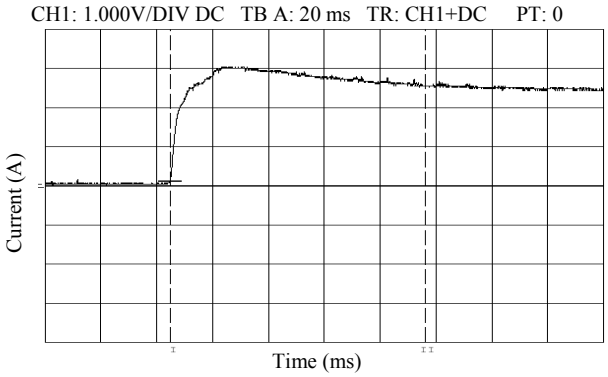


Fig. 13 The transient response of the conventional power supply system at 6A

Fig. 13 shows the waveform for the transient response of the conventional power supply system where the system responds slowly. From this figure it is observed that the system has underdamped response with about 20 % overshoot and 70 ms settling time. It is clear the system has a delay caused by the analog components of the conventional power supply system. Fig. 14 shows the waveform of load current in steady state. Measurement shows that ripples were neglected due to the series choke inductance in the LC- filter.

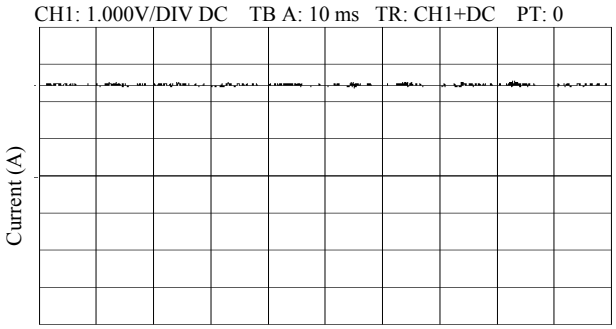


Fig. 14 The steady state load current of the conventional system at 6A

*B. Transient Response of the Step-Down Chopper*

Fig. 15 shows the waveform of the transient response of the buck chopper using PI- controller and the designed parameters $k_P = 3$ and $k_i = 500$ from the simulation results. The reference current is 4.0 A. This figure shows critically damped response with 3 ms rise time. The proposed system offers high performance in the transient state. Therefore this performance is much better than that of the conventional system. The steady state error is zero due to the integral term in the PI-controller and the ripple content in the same order of magnitude as that of conventional system because of the high switching frequency. Table I shows comparison between the new system and the conventional system to show the gained improvements.

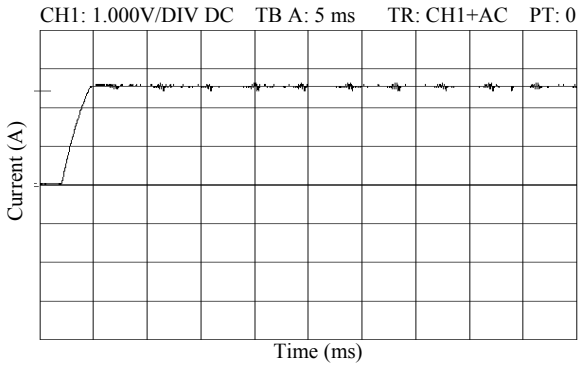


Fig. 15 The transient response of the chopper

TABLE I
COMPARISON BETWEEN THE NEW SYSTEM AND THE CONVENTIONAL SYSTEM

| | The rise time | The settling time | Overshoot |
|---|---|---|---|
| The new system | 3ms | zero | zero |
| The conventional system | 3ms | 70ms | 20% |

### C. *Steady State Response of the Step down Chopper*

Since the performance of the current source depends not only on the controller parameters but also on the connected loads extensive tests were made on the new system changing the load inductance with the same time constant. Fig. 16 shows the steady state response of the new system with the same load L = 5 mH and R = 1.1 ohm at 4A and the load is doubled in fig. 17. It is clear by comparison between the two figures the ripples have eliminated in fig. 17.

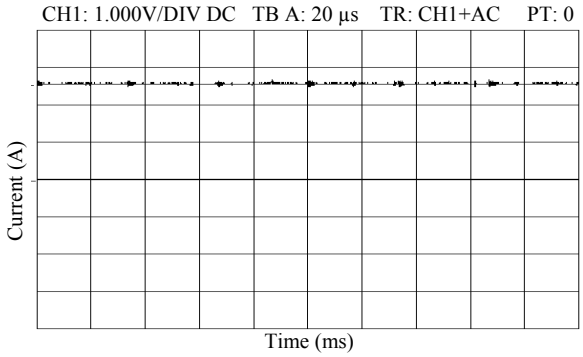


Fig. 16 The steady state response at load R=1.1 ohm and L= 5 mH

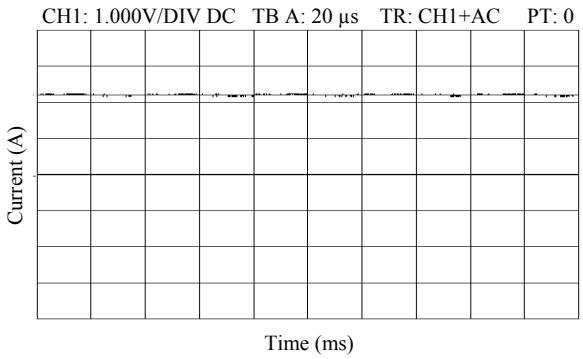


Fig. 17 The steady state response at load R=2.2 ohm and L= 12 mH

## VI. CONCLUSION

From the obtained results we can state that: The implemented system offers a good transient and steady state response where the digitally controlled current source can provide a very fast response, while, at the same time, retaining all the advantages of a digital design and the model of four quadrant chopper, used in the design of the system, predicts correctly the system transient behaviour. The load inductance is an important factor in the reduction of ripples in the load current. Therefore, the dc-dc chopper and the DSP based control and monitor system represent the best upgrading scheme for the bulky and troublesome conventional system used.

## ACKNOWLEDGMENT

The authors would like to express their thanks to Prof. Dr. Usama Seddik, director of Cyclotron Project for his support and acknowledge the financial support of the cyclotron project in the Egyptian Atomic Energy Authority (EAEA).

## REFERENCES

[1] A. Azzam," Factory tests of the physical parameters of the MGC-20 cyclotron," *Internal Report no. 306* (1999), Nuclear Physics Dept, Nuclear Research Centre, Egyptian Atomic Energy Authority (EAEA).
[2] "Cyclotron MGC-20 Operating and User Manual," D.V. Efremov Scientific Research Institute of Electrophysical Apparatus (NIIEFA), Saint Petersburg, Russia.
[3] M. Adel,"Design and implementation of microcontroller 80196 based PWM boost rectifier," *Master of Science thesis*, Benha University, Benha, Egypt 2006.
[4] P. C. Todd, " Snubber Circuits: Theory, Design and Applications," Unitrode Corporation, May 1993.
[5] B. W. Williams, " Power electronics: Devices, Drivers, Applications and Passive Components," The Macmillan Press L.T.D., London (1994).
[6] Motorola DSP56F807 Family Manual Rev. 3, Dec. 2003.
[7] Motorola DSP56F807 User Manual, Rev. 4, 2003.
[8] S. D. Markande, P. M. Joshi and S. K. Katti,"Microcontroller based temperature controller implementation of fuzzy logic," *The Institution of Engineers (India) Journal,* vol. 85, p. *7, May 2004*.
[9] F. Mihalic and D. Kos, ""Randomized PWM for conductive EMI reduction in DC-DC choppers," *HAIT Journal of Science and Engineering* B, vol. 2, issues 5-6, pp.594-608, 2005.
[10]F. Bertling and S. Soter, "Increasing efficiency of an DSP- controlled converter by on the fly changing of the gate drive method," *PESC04* Aachen, Germany 2004.
[11]J. Murphree, B. Brzezinski and J. K. Parker," Using a fixed point digital signal processor as a PID controller," *Proceedings of the 2002 American Society for Engineering Education Annual Conference & Exposition,* Session 2359. Abuquerque, NM
[12] G. Olivier, V. R. Stefanovic and M. A. Gamil," Digitally controlled thyristor current source", *IEEE Transactions on Industrial Electronics and Control Instrumentation*, vol. 26, no. 3, p. 185, August 1973.